Nuclear and magnetic medium-range order in rare-earth-based amorphous alloys

1991 J. Phys.: Condens. Matter 3 2207

(http://iopscience.iop.org/0953-8984/3/14/001)

J. Phys.: Condens. Matter 3 (1991) 2207–2229. Printed in the UK

REVIEW ARTICLE

Nuclear and magnetic medium-range order in rare-earth-based amorphous alloys

B Boucher† and P Chieux‡

† Service de Physique du Solide et de Résonance Magnétique, CEN Saclay, F-91191 Gif-sur-Yvette Cédex, France

‡ Institut Laue–Langevin, 156 X, F-38042 Grenoble Cédex, France

Received 29 May 1990, in final form 24 January 1991

Abstract. This review gathers the results of studies performed on the medium-range order (MRO) of rare-earth-based amorphous alloys. It presents some macroscopic properties characterizing the alloys (susceptibility, magnetization, characteristic temperatures, etc.) and the results obtained by small angle neutron scattering (SANS), the only technique used to determine the nuclear or magnetic medium-range order. We review predictions concerning these medium-range orders, including segregation (Guinier law) and nuclear or magnetic fluctuations (Ornstein–Zernicke law, correlated spin glass and ferromagnet wandering axis model).

It describes the difficulties associated with the interpretation of SANS results and the present limits of the data analysis. The various results describing the nuclear and magnetic medium-range order are then given and discussed.

1. *Introduction*

The macroscopic properties and the nuclear or magnetic short-range order (SRO) of amorphous alloys have been extensively studied (Chappert 1982). In contrast, the medium-range order (MRO) which is nevertheless essential for a complete understanding of these systems has received less attention. Here we review the nuclear and magnetic MRO of rare-earth (RE) alloys. We limit the choice mainly to the heavy RE (Gd, Tb, Dy, Ho, Er) and occasionally the Nd alloys because these have been systematically studied and, except for Nd which has a small moment and Gd which is an isotropic S ion, they present both a large magnetic moment (between 7 and 10 μ_B/RE) and a high magnetic anisotropy. The comparison of the macroscopic properties of these different systems has clarified the role of exchange and that of anisotropy. Harris *et al* (1973) have explained the magnetic behaviour of RE amorphous alloys with a 'random anisotropy model' in which the local anisotropy defines the axis of the moments on a site and the exchange its direction.

Two kinds of alloys can be distinguished, alloys with the RE as the only magnetic ion and those with two magnetic ions (RE and 3d ions). This distinction is a practical one, corresponding to different magnetic orders (aspero- or speri-magnetic SRO, respectively) and to different ordering temperature ranges. In only the first case is the nuclear order easily determined by neutron scattering without the risk of crystallization because the magnetic ordering temperature is then low (< 300 K).

0953-8984/91/142207+23$03.50

The main magnetic properties of these amorphous alloys can be summarized as follows. The reciprocal susceptibility, when it is possible to measure it without sample cristallization, i.e. for alloys having a low ordering temperature, does not exhibit a particular temperature dependence above the ordering temperature. Except for some light RE (Pappa and Boucher 1980) it has a linear paramagnetic part, with a normal effective moment and an asymptotic Curie temperature θ, which is clearly positive, pointing to the predominance of positive magnetic interactions. However, the deviation from the Curie law on a large temperature range, say roughly for $\theta < T < 2\theta$ (figure 1), may be related to traces of local magnetic order above the ordering temperature (usually called T_c or $T_f \sim \theta$) giving rise to coherent neutron scattering at small angle as we will see. With an applied field, the magnetization varies greatly depending on whether a zero-field-cooled (ZFC) or field-cooled (FC) procedure is followed below a field-dependent temperature T_f, for which the susceptibility presents a cusp as for a spin glass in low field (figure 2).

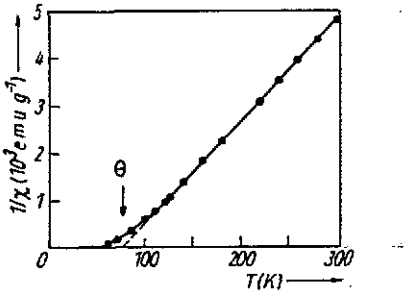

Figure 1. a-$Tb_{52}Ag_{48}$. Reciprocal susceptibility versus temperature. The values of θ is well defined, but this curve cannot lead to a value for T_c (Boucher 1977).

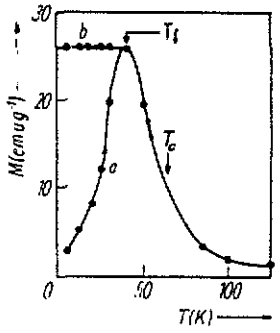

Figure 2. a-$Tb_{52}Ag_{48}$. Temperature dependence of the magnetization in an applied field of 1 kOe. Curve a, ZFC sample; curve b, FC sample (Boucher 1977a). T_f corresponds to the branch separation. T_c as determined by an Arrott plot is shown in the figure.

As a matter of fact, several temperatures have been introduced in the literature to characterize magnetic ordering in these amorphous alloys. We find:

(i) the asymptotic Curie temperature θ (figure 1);

(ii) the critical Curie temperature T_c generally determined by an Arrott plot (see Aharony and Pytte 1980);

(iii) the field-dependent temperature of the susceptibility cusp T_f;

(iv) the magnetic ordering temperatures as obtained from measurements such as small angle neutron scattering (SANS) (Boucher *et al* 1986, Hasanain *et al* 1986).

Since the various techniques probe the sample differently, they do not converge to a unique ordering temperature. In practice T_c or T_f are often rarely used, as the existence of a critical temperature is still controversial.

Another property of RE alloys is given in figure 3, which represents the reduced isothermal magnetization versus very intense field (up to 40 T). Fields of 13 T are necessary to saturate the Gd alloy (Gd is a S-state ion) proving the existence of anti-

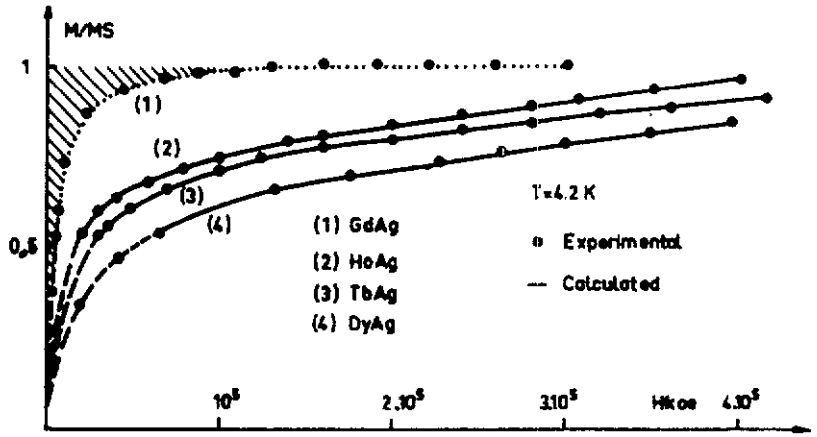

Figure 3. Reduced magnetization in high applied field at 4.2 K (Boucher 1977b). GdAg reaches saturation value for $H = 13$ T because of antiferromagnetic interactions.

ferromagnetic interactions that contribute to magnetic disorder. For the other alloys local anisotropy prevents saturation from being reached.

As far as the microscopic structure is concerned, the amorphous alloys are metastable phases obtained only by rapid quenching; thus some frozen-in compositional disorder or aggregates leading to a coarse structure or medium-range order (MRO) is to be expected. The magnetic order itself is already influenced by the equilibrium topological and chemical SRO which strongly perturb the magnetic exchange and disperse the local anisotropy axis, leading to moment dispersion. This phenomenon will be modulated by the above non-equilibrium medium-range composition variations (MRO). It is therefore necessary to characterize the magnetic MRO and see how it is modified by an applied field or affected by other treatments such as surface effects.

The medium-range order can be obtained from electron microscopy, small-angle scattering of x-rays (SAXS) or of neutrons. Apparently one study has been made by electron microscopy (Wang Zhenxi *et al* 1988) on Nd, Fe, Co and B amorphous alloys and does not provide evidence for composition fluctuation or segregation. Few studies have been performed by SAXS (e.g. Flank and Naudon 1980). In this case, the difficulty comes from the excessive values of the accessible momentum transfer ($q = 4\pi \sin\theta/\lambda$, where 2θ is the scattering angle and λ the wavelength) which allow us to see only small clusters. Very profitable use could nevertheless be made of anomalous x-ray scattering, but this techique has not yet been used for RE based amorphous samples. However, when the magnetic properties are investigated, SANS is mandatory and has been widely used; SANS is able to reveal the nuclear and magnetic MRO from q values as low as 10^{-3} Å^{-1} or even less in particular cases (Tomimitsu *et al* 1986) and up to 0.5 Å^{-1}, corresponding to structures in the range 10 to 3000 Å. The weak absorption of the neutrons even for wavelengths as large as 10 Å facilitates the use of cryostat and thick samples (0.02–0.5 mm). At high temperature, well above the magnetic ordering temperature the nuclear incoherent and paramagnetic scattering contribute to the background and are easily calculated; only the nuclear order participates to the scattering pattern. Below the ordering temperature both the nuclear and magnetic order contribute to the scattering pattern, the disordered moments contributing to the

background. Since in an amorphous system, the nuclear order is nearly temperature independent, the magnetic scattering is obtained from the difference of two patterns taken below and above magnetic ordering temperature. Therefore SANS provides both the nuclear and magnetic scattering. Moreover it is possible to obtain the intensities with an absolute scale by, for example, normalization to the scattering of a vanadium sample. The cross section determined can be very large: 10^6–10^8 b/molecule. The contrast $K(r)$ (the difference of the scattering length per unit volume for two volumes distant by r, $(b_1/v_1) - (b_2/v_2)$) is also obtained and allows the amplitude of the composition and magnetization fluctuations to be obtained.

We recall some theoretical models (section 2) before reviewing (section 3) and discussing (section 4) the experimental results.

2. Theoretical models for MRO

2.1. Nuclear order

In a liquid far from critical points, there is no long-range fluctuation, but if on quenching it passes close to an immiscibility gap or enters an unstable state, then fluctuations or heterogeneities might be frozen in. Therefore in amorphous alloys we might expect at small angles either a Guinier scattering law ($\exp(-\alpha q^2)$) corresponding to microsegregation or an Ornstein–Zernicke Lorentzian (denoted by L) corresponding in real space to composition fluctuations described by a distribution $(1/\sqrt{r})\exp(-r/\xi)$ with correlation length ξ. These fluctuations, which are normally simple atomic composition fluctuations could also be fluctuations of special atomic arrangements (Dubois 1988) with corresponding local symmetry axis correlations detectable, in the case of magnetic systems, as correlations between the easy magnetization axis (Boucher *et al* 1979 a,b).

The amorphous state could also present self-similar or fractal order, i.e. the scattering curve could have a non-integral power law form with exponent values between -2 and -4, depending on the predominance of bulk or surface (or interface) effects. Indeed such a behaviour is often found, at least for some part of the scattering pattern; however, most authors, including ourselves, have preferred to describe the results with the help of classical models which are just as powerful and have always given very reasonable physical values for the scattering length per unit volume.

2.2. Magnetic order

The existence of amorphous magnetic alloys raises two fundamental questions, in the case of disordered systems: is there an infinite ferromagnetic cluster and is it possible to define a magnetic critical temperature? Several theoreticians have attempted to solve these problems (Imry and Ma 1975, Aharony and Pytte 1983, Fischer 1987, Chudnovsky 1988) and they are in good agreement in affirming that from scaling law arguments, there is no infinite cluster for dimensionalities $d \leqslant 4$. Two cases have been considered; the magnetic order is due either to random exchange only, creating on each site a random field (random field model, RFM), or to random anisotropy in the presence of ferromagnetic exchange (random anisotropy model RAM). Aharony and Pytte (1980) show that for the RAM, there exists a critical temperature T_c, where the magnetic susceptibility diverges, although there is no long-range order (the magnetization goes to zero with the field). They describe the corresponding Arrott plots; for the RFM

they find only a freezing temperature with relaxation phenomena, as is the case for a spin glass under low applied field.

The existence of a critical temperature is not very clear, as is revealed by the vocabulary used for describing the experimental results, but in all cases there is a magnetic MRO at low temperatures. Authors have tried to predict this order in the RAM with weak anisotropy and to obtain the magnetic correlation function at low temperature. From scaling laws, they predicted a power law of the form q^{-N}, for magnetic SANS (Aharony and Pytte 1980). Then, by analogy with spin glasses, a correlation function exponentially decaying with distance and leading in reciprocal space to a Lorentzian-squared (L^2) scattering law was introduced (Aharony and Pytte 1983, Fischer 1987, Chudnovsky *et al* 1986). This correlation function is written as

$$M_0^2\langle\sigma_1(r_1)\sigma_2(r_2)\rangle \propto \exp(-|r_1 - r_2|/\xi)$$

where ξ is the correlation length, σ_i the spin, M_0 the magnetization. Fourier transforming gives

$$A/(q^2 + 1/\xi^2)^2 = L^2$$

with $A \propto M_0^2/\xi$. Moreover, the spin waves or residual fluctuations of spin lead to a supplementary term $L' = B/(q^2 + 1/\xi^2)$, a dynamic term implying that B decreases with T. Thus the scattered intensity can be described by $L^2 + L'$. Fischer (1987) reaches the same conclusion from a slightly different calculation. Chudnovsky (1988) shows also how ξ depends on exchange, anisotropy and magnetization and demonstrates that ξ is strongly influenced by the correlation between anisotropy axis. We will see that the magnetic scattering can often be fitted by an $(L^2 + L')$ expression, but that L' does not show the temperature dependence expected for a dynamic term, namely B decreasing as the magnetization squared with T increasing (Rhyne 1986).

The exponential law chosen for the correlation function between spins leads to a model called 'correlated spin glasses' (CSG) in which, the net magnetization is zero, the spins being ferromagnetically correlated at small distances but progressively rotating when the distance increases (figure 4(*a*)).

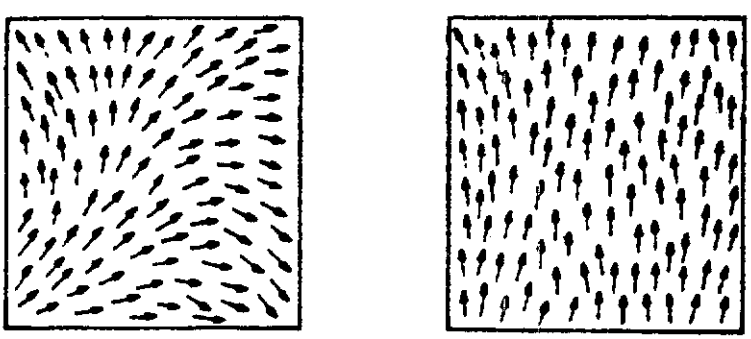

Figure 4. Atomic spins in a ferromagnet with weak random anisotropy. (*a*) correlated spin glass (CSG); (*b*) ferromagnet with wandering axis (FWA) (Chudnovsky 1988).

On applying a magnetic field, this structure is modified and the correlation length ξ increases, the field tending to align the moments which remain, however, influenced by anisotropy. Thus the net magnetization is, in that case, no longer zero; Chudnovsky *et al* (1988) describe the system as a 'ferromagnet with wandering axis' (FWA) (figure 4(*b*)) and characterize the disorder by a correlation function between the spin components perpendicular to the field direction, which decays exponentially with distance. The scattered intensity should then vary as a Lorentzian-squared with correlation length $\xi_T(\neq \xi)$. Its dependence on applied field should be as $H^{-1/2}$ since the magnetization varies as $\partial M/M_0 \sim H^{-1/2}$ at the approach to saturation.

To summarize, at low temperature ($T \ll T_c$) for $H = 0$ we expect a scattering of the type $L^2 + L'$, both terms having the same correlation length ξ. For $H \neq 0$, we still expect a L^2 term but with a correlation length $\xi_T(\neq \xi)$ characteristic of the disorder of the transverse spin components. For high temperature ($T > T_c$) Fischer (1987) shows that the spin fluctuations give a Lorentzian scattering law as for an ideal ferromagnet in the paramagnetic phase plus a Lorentzian-squared term which exists only for $H \neq 0$.

3. Experimental results

3.1. Preliminary remarks on data analysis and implied models

The experimental results on MRO come from SANS measurements. It is very important to keep in mind that these measurements always have a $q_{\min}$ limit which depends on the chosen instrument. This implies that corresponding fluctuations or aggregates of sizes of order $2\pi/q_{\min}$ and above are undetectable, although they might be present in the investigated system. Obviously, the experiments should be performed on the largest possible q range, such as to cover a large domain of real space fluctuations. However, this often implies added complexity in the data analysis since a unique model will rarely apply to the whole range and combination of models applying to different parts of the pattern, will be necessary.

The various models which have been developped to interpret the magnetic SANS of amorphous alloys correspond to different analytical expressions which must be fitted to the scattering curves. We could therefore by careful comparison with good data sets hope to decide, from the experiment itself, about the most appropriate model. However, although high statistical accuracy and large q range have been achieved for a system like $Tb_{22}Cu_{78}$ (figure 6 later), it remains very difficult to distinguish on a numerical basis between scattering laws of the type $L^{N/2}$ and of the type q^{-N} (with $N = 2, 3$ or 4). It is only when a saturation of the scattering curve is detected at low q values (such as that observed for ZFC $Tb_{65}Cu_{35}$, see figure 11 later) that the Lorentzian description can be preferred.

Another situation is found with the $L^2 + L'$ functions

$$L^2 + L' = A/(q^2 + 1/\xi^2)^2 + B/(q^2 + 1/\xi^2)\,.$$

In that case, depending on the q range chosen, and on the value acceptable for ξ (which might strongly depend on parameters such as T, H, etc.), the description might as well reduce to a single L^2 or L' term (we see in figure 5 that at high q values, we have only a L' term). The same difficulty occurs if one wishes to observe a crossover between a q^{-4} and q^{-3} law (Boucher *et al* 1979b). In other words we are faced with the

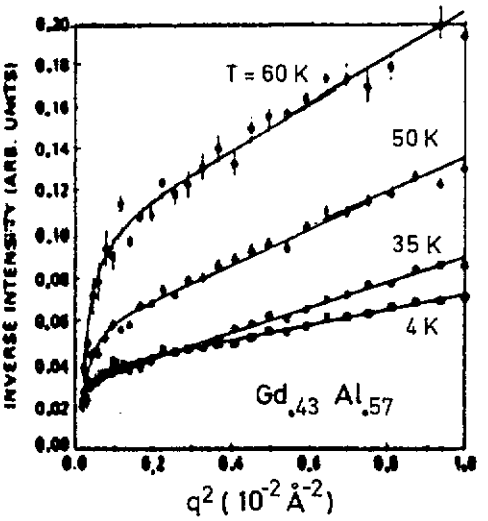

Figure 5. a-$Gd_{43}Al_{57}$. Inverse intensity versus q^2 (inset of figure 2 of Spano *et al* (1987)). We can see the existence of the L' term, but at low q values another term is predominant.

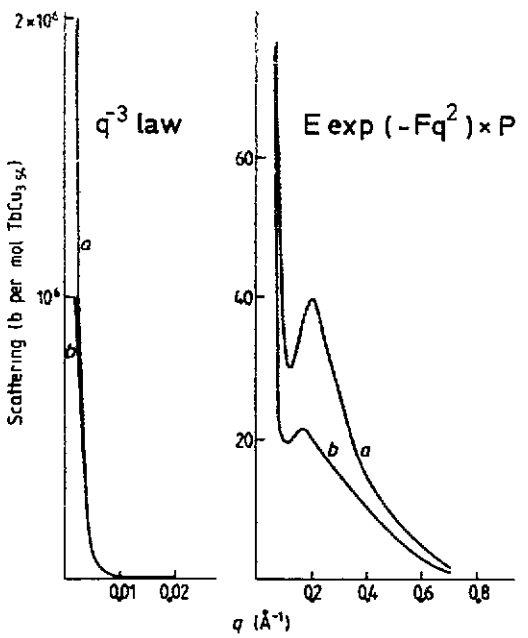

Figure 6. a-$Tb_{22}Cu_{78}$. Typical nuclear scattering pattern taken at 300 K. Curve a, annealed sample; curve b, as-cast sample. For high q values (right-hand graph) we observe a ring with $\sigma_{max} \sim 40$ b/$TbCu_{3.54}$; for low q values (left-hand graph) the scattering follows a q^{-3} law. At q_{min} the scattering reaches a few 10^6 b/$TbCu_{3.54}$ (Boucher *et al* 1983).

unpleasant situation that optimization of the experimental conditions depends on *a priori* knowledge of the magnetic correlation length and correlation function.

In the general case, when a large q range has been investigated we might have to fit three terms such as L^2, L' and $\alpha\exp(-\beta q^2)$, with two adjustable parameters each. Then the data analysis essentially relies on the assumption that the most characteristic parts of the scattering curve are each dominated by only one of these terms (see ZFC $Tb_{65}Cu_{35}$ at 4 K, see figure 11 later). Absolute measurements are then very important to cross check if the various parameters (such as the scattering contrasts) are in agreement with the sample characteristics.

In the case of a q^{-N} power-law description of the scattering, an integral value is not always found for the exponent. Whether this implies a fractal behaviour of the system is a matter of conjecture, especially if only a rather narrow q range is covered. As a matter of fact an alternative description has often been successfully tried with a $L^{N/2}$ law ($N = 2, 3, 4$). Generally speaking, all laws in q^{-N} observed for the RE alloys can be considered to be limiting values of $L^{N/2}$ laws ($N = 2, 3, 4$) with $1/\xi$ much smaller than q_{min}. This is probably why the two descriptions are equivalently found in the literature, N being generally independent of temperature except for $ErCo_2$ (Boucher 1979b) where $N \sim 4$ at 4 K and increases with T. However, the models implied by these two descriptions are quite different. For example a q^{-4} behaviour (Porod law) could be interpreted as being due to sharp boundaries between domains, while L^2, which Fourier transforms in an exponential (table 1), would come from rather smooth fluctuations. Also there is no real criterion to completely exclude fractal behaviour.

Table 1. Scattering laws and their corresponding contrast variations. σ is the cross section of isotropic scattering expressed in b or μ_B^2 per formula unit. Assuming the scattering is due to static order, the Fourier transform gives the squared contrast $K^2(r)$; $K(r) = (b_1/v_1 - b_2/v_2)\sqrt{v}$ is the difference between the scattering length per unit volume for two volumes (v_1, v_2) spaced by r and rescaled to a formula unit volume (v). A, B, C, E and F are constants.

σ	$K(r)$
$A/(q^2+\kappa^2)^2$	$(Av/32\pi^2\kappa)^{1/2}\exp(-\kappa r/2)$
$A/(q^2+\kappa^2)^{3/2}$	$(Av/(2\pi)^3)^{1/2}\,(K_0(\kappa r))^{1/2}$
$A/(q^2+\kappa^2)$	$(Av/16\pi^2)^{1/2}(1/\sqrt{r})\exp(-\kappa r/2)$
$B\exp(-Cq)$	$(2BCv/(2\pi)^3)^{1/2}/(r^2+C^2)$
$E\exp(-Fq^2)$	$(Ev/32\pi^{5/2}F^{3/2})^{1/2}\exp(-r^2/8F)$

Having emphasized the difficulties of the data analysis and the lack of specifity of some model descriptions if they do not fully integrate all the investigated sample characteristics, it is time to see what can be really obtained from MRO studies.

Whatever the chosen model it is always possible to reach limiting values for some fundamental parameters as the correlation length or domain size, the composition and magnetization fluctuation profile, the contrast for scattering. We point out that since the magnetic scattering depends on the magnetization, i.e. on two parameters, a magnitude and a direction, small local perturbations of the direction could have a strong influence and could be easily detected.

For RE alloys, all the authors have assumed that the observed SANS was due to the bulk properties of the materials and all the models for magnetic MRO are based on this assumption. By using the immersion method, which allows one to match the surface

scattering of the sample with a solvent, and which thus suppresses sample surface effects, we have ourselves verified with $Tb_{65}Cu_{35}$ that most of the scattering curve indeed came from the bulk (Boucher *et al* 1989). Of course, the immersion method, in which the H/D ratio in solvent mixtures (such as water–methanol or methanol–glycerol) is varied to match the sample surface scattering, can only be used near room temperature; i.e., for RE alloys with one magnetic ion the method cannot be applied to the magnetic part of the scattering. However, all measurements performed by us on an absolute scale gave very realistic physical values for the various parameters without the introduction of surface effects. These results are in agreement with those of Maret *et al* (1988) on NiY, but contrast with those obtained on $Pd_{80}Si_{20}$ (Rodmacq *et al* 1985) or more recently $Fe_{80}B_{20}$ (Lamparter and Chieux private communication) where the influence of surface effects on the scattering are very important.

3.2. RE alloys studied by SANS

The following alloys with only one magnetic RE ion have been studied by SANS: Tb_xCu_{1-x} ($0.18 < x < 0.65$) (Boucher *et al* 1983, 1986, 1988a, b, 1990, Guimaraes *et al* 1987), $Er_{0.69}Cu_{0.31}$ (Boucher *et al* 1988b, 1990) Tb_xSi_{1-x} ($0.18 < x < 0.87$) (Simonnin *et al* 1984, 1985). DyCu (Pickart *et al* 1984, Hasanain *et al* 1986), GdAl (Spano *et al* 1987, Spano and Rhyne 1987).

In most of these alloys both nuclear and magnetic MRO have been investigated because the magnetic ordering temperature is below room temperature and it is possible to measure the nuclear scattering without activating the ionic mobility. This is not the case for the alloys with ferromagnetic ions (RE–3d) such as Tb_xFe_{2-x} ($0.02 \leqslant x \leqslant 0.75$) (Rhyne *et al* 1974, Pickart *et al* 1974, Rhyne and Glincka 1984, Spano and Rhyne 1985, 1987), $REFe_2$ (RE ≡ Er, Ho, Nd) (Spano and Rhyne 1988, Spano *et al* 1985, Hasanain *et al* 1986, Alperin *et al* 1979) $ErCo_2$ (Boucher *et al* 1979a, b).

3.3. MRO in alloys with only one magnetic ion

In the following, we shall review all the data for amorphous alloys with one magnetic RE ion with more details for Tb_xCu_{1-x}, which seems a typical case.

3.3.1. Nuclear order. The nuclear order has been studied at 300 K for all samples indicated in the list above, except Gd Al and Dy Cu.

Figure 6 shows a typical pattern which has been obtained for $Tb_{0.22}Cu_{0.78}$. At high q values we observe a diffusion ring characteristic of small inhomogeneities (~ 10 Å) regularly distributed (~ 50 Å) over the sample. The scattering level corresponds either to considerable local composition variations (8–10% of the dominant atom concentration) or to the segregation of one constituent. In $Tb_{0.22}Cu_{0.78}$ small aggregates or 'bubbles' of Tb have been identified (Boucher *et al* 1986) by magnetic SANS. Annealing increases the size of these aggregates or concentration fluctuations (Boucher *et al* 1986, 1988a).

At low q values the scattering is fitted by a q^{-N} law with $N = 3$ or 4 depending on x. These results can be interpreted by the existence of 'atomic domains' with a size of a few thousand Angström with constant scattering length per unit volume (b/v) but having slightly different scattering values from one domain to another ($N = 4$) or due to domains with b/v values that vary rather sharply at the approach of the domain boundaries ($N = 3$) (figures 7(a) and 7(b)). It is also possible to consider the q^{-N} scattering law as a limiting expression for a $L^{N/2}$ law having a large correlation

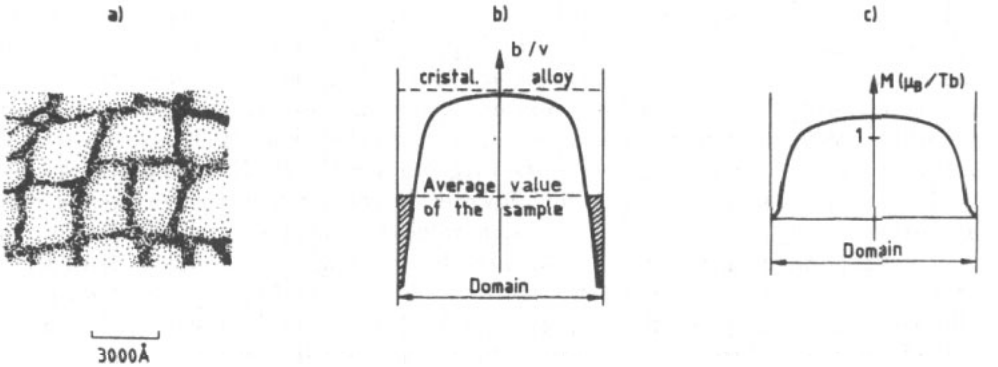

Figure 7. Schematic drawing of the scattering length (or magnetization) profile across a domain, as deduced from: (*a*) a q^{-4} nuclear or magnetic scattering law; (*b*) a q^{-3} nuclear scattering law; (*c*) a q^{-3} magnetic scattering law (Boucher *et al* 1983, 1986).

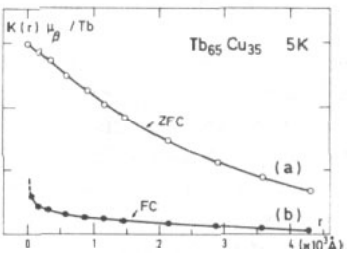

Figure 8. Variation with distance r of the scattering length per unit volume obtained from: curve a, a Lorentzian-squared scattering law, $K(r) = (Av/32\pi^2\kappa)^{1/2}\exp(-\kappa r/2)$; curve b, a Lorentzian to the power 3/2, $K(r) = (Av/(2\pi)^3)^{1/2}K_0^{1/2}(\kappa r)$; K_0 is a modified Bessel function. For nuclear or magnetic scattering on an absolute scale, the coefficient multiplying K_0 is much smaller than the coefficient for the exponential function, but in the two cases the variation of the contrast with r is not very different except at low values of r. This variation has to be compared with the contrast variation deduced from q^{-N} laws given in figure 7.

length. Then the b/v varies exponentially with distance ($N = 4$) or as a square-root modified Bessel function ($N = 3$) (see examples in figure 8).

Thus, depending on the scattering law chosen, we have several possible descriptions

(i) (q^{-N}, $N = 4$). There are domains in which the composition is constant but varies from one domain to another;

(ii) ($L^{N/2}$, $N = 4$; $L^{N/2}$, or q^{-N}, $N = 3$). There is a variation of contrast within the domains; from the centre of the domain to its border, the contrast profile depends on the scattering law chosen, but there is always a large area in which the variation is weak and a region in which it is much stronger. It is difficult to define with certainty the origin of the variation of b/v. We may think of composition variation of a few per cent with or without a gathering of impurities or aggregates along the domain boundaries, density variation being excluded (see e.g. Lamparter and Steeb 1988). This proposed solution accounts for the measured absolute intensities and gives quite reasonable values for the spatial variations of the physical parameters. For example,

the as-prepared $Tb_{22}Cu_{78}$ sample (Boucher *et al* 1983) shows a b/v maximum variation of 0.003×10^{-12} cm Å^{-3} which corresponds to a maximum concentration variation of 7% in Cu content (neglecting any impurity effects). Similar proportions are obtained for numerous amorphous alloys.

Usually, samples with a single magnetic ion were prepared by sputtering. The $Tb_{0.65}Cu_{0.35}$ samples were also prepared by both sputtering and flow casting and give the same type of scattering, that is a diffusion ring and a q^{-N} law. Thus these properties are independent of preparation method and are related to the type of alloy.

We will see that the magnetic scattering obeys the same laws.

3.3.2. Magnetic order. Magnetic MRO gives rise to an important isotropic scattering which is several times more intense than the nuclear SANS. A typical pattern (chosen from $Tb_{22}Cu_{78}$) is represented in figure 9. A combination of several scattering laws is needed to fully describe it, such as given by a relation of the type

$$\sigma = A/q^3 + B\exp(-Cq) + E\exp(-Fq^2)P \tag{1}$$

where A, C, E and F are constants, B is generally constant and P is an interference function. However, each of these laws applies only to a restricted part of the pattern and the constants satisfy reasonable values for the scattering contrast which in the present case is related to the magnetization per unit volume, with the reference volume adapted to the q range considered. Moreover it is important to note that the analysis takes benefit of what has been learned from the nuclear structure, for example the geometrical parameter (F and P in equation (1) above) related to the distribution of aggregates will remain unchanged.

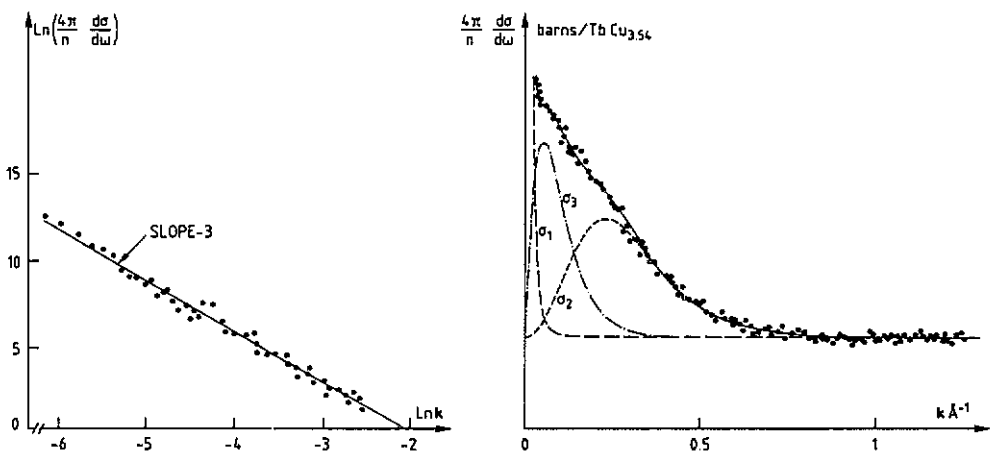

Figure 9. a-$Tb_{22}Cu_{78}$. Magnetic cross section at 2.6 K (annealed sample) in b/$TbCu_{3.54}$ versus q. Log–log plot (left-hand graph); $\sigma(q)$ plot (right-hand graph). Full circles, experimental values; full curves, calculated values with relation (1); broken, dotted and chain curves, calculated σ_i components of the cross section (Boucher *et al* 1986).

The scattering at the lowest q values is interpreted as a set of large magnetic domains ($\sim 10^4$ Å) carrying a magnetization which varies at the approach to the

domain boundaries (q^{-3} law) by a few tenths of a Bohr magneton per Tb atom. Alternatively it can be described as magnetization fluctuations with a large correlation length ($L^{3/2}$ law). In both description the real space distribution of the scattering length per unit volume contains a steeply and a slowly varying part as shown in figures 7(*b*), 7(*c*) and 8(*b*).

At the larger q values as already observed for nuclear scattering we obtain a Guinier law ($\exp(-Fq^2)$ term) and an interference ring characteristic of a distribution of small aggregates (size $\sim$ 10 Å, intercluster spacing $\sim$ 50 Å). The corresponding scattering contrast permits to identify terbium aggregates carrying a large magnetization of a few Bohr magnetons per Tb atom.

In the intermediate q range it remains a signal which cannot be described by the above laws. This signal has been shown to obey a $\exp(-Cq)$ law corresponding to a real-space Lorentzian distribution. This has been interpreted by the scattering from the region around the aggregates which carries an intermediate magnetization due to the coupling between that of the aggregates and the matrix. This term is a static term. The width at half maximum of the Lorentzian (25 Å) gives an idea of the extension of this coupling.

This distribution of magnetization over sizes from 10 to a few thousand angstrom, which is in part schematically represented in figure 10, has been called 'seedy magnetic order' (Boucher *et al* 1986a). We note that the magnetization distribution is highly inhomogeneous, the 'bubbles' occupying 7–8% of the total sample volume and carrying 50% of the magnetization. Although the scattering laws which have been introduced are still somewhat conjectural, this parametrization gives a detailed description of the magnetic behaviour (size (or correlation length) and magnetization of domains, size and magnetization of local heterogeneities, coupling between 'bubbles' and domains).

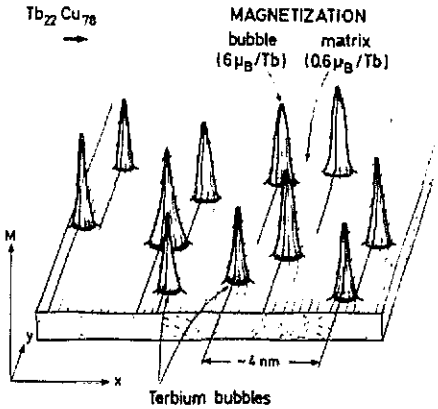

Figure 10. Schematic representation of 'seedy magnetic order'. In a weakly magnetized domain, of which one part only is represented, we observe some very intensely magnetized peaks, whose magnetization decreases progressively down to the domain magnetization ($\exp(-Cq)$ scattering law). At low temperature the magnetizations of different parts of the sample are coupled between them (Boucher *et al* 1986, 1988c).

This semi-microscopic, or mesoscopic, description of the magnetization distribution permits to consider several magnetic orderings up to 4θ, the asymptotic Curie temperature θ being at 27 K. Below θ the magnetizations of the domains are coupled with each other and the aggregate magnetizations are coupled with those of the

domains. Between θ and 2θ the interactions between domains vanishes progressively as the scattering at very low q values. At 2θ the magnetization of the aggregates is still present, and will be detectable as a Guinier law up to 3θ or 4θ (Boucher *et al* 1986). Of course, this shows how difficult it will be to define macroscopic ordering temperatures in this system.

We shall now detail several systems which present characteristic properties.

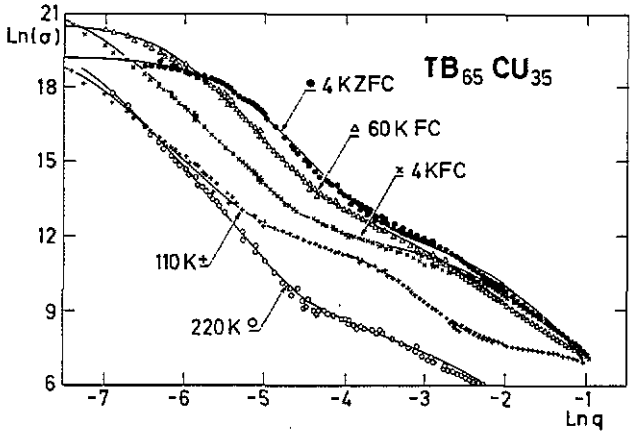

Figure 11. Logarithmic representation of experimental magnetic cross section σ measured in a plane perpendicular to the applied field; the curves are calculated by relations (2) and (3) (table 2 caption). The FC samples are cooled in an applied field to 4 K and then heated up to 220 K in zero field. The patterns evolve towards ZFC for $T > 20$ K (see e.g. the 60 K curve) (Boucher *et al* 1989b).

The study of $Tb_{65}Cu_{35}$ (Boucher *et al* 1988b, 1990) gives very interesting results. In this system at 4 K, we find for magnetic scattering (ZFC, 4 K), evidence for a Lorentzian-squared magnetic scattering (L^2) (figure 11) with correlation length ξ ($= 1/\kappa \sim 240$ Å) which is proved by the leveling-off of the scattered intensity for $q \leqslant 7 \times 10^{-3}$ Å. With applied field (FC sample) the scattering is slightly non-isotropic (as in figure 14(a) later), and in contrast to theoretical predictions which lead to a L^2 behaviour (subsection 2.2), the scattering law becomes $L^{3/2}$ with a considerable increase of ξ (see figure 11). In the direction perpendicular to the field, the value of ξ_T (~ 1400 Å) is then equal to that obtained for nuclear scattering at 300 K (see table 2). The magnetization varies sharply at short distance, but since the field aligns the local magnetizations, it remains nearly constant over large distance (see figure 8) with an average domain value of about 3.8 μ_B per Tb atom (Boucher *et al* 1988b). Above the magnetic transition (~ 90 K) and up to about 200 K for ZFC and FC samples, we observe a remaining weak magnetic scattering still described by a $L^{3/2}$ law and with correlation length equal to the nuclear correlation length.

Thus we can say that in this system the medium-range magnetic order, in the absence of field (ZFC) is governed by magnetic parameters (anisotropy, exchange, etc.), while in the field-cooled case (FC) the nuclear order fixes the magnetic order to the nuclear domain size (~ 1 μm).

The study of $Er_{69}Cu_{31}$ (Boucher *et al* 1988b, 1990a) and Tb_xSi_{1-x} (Simonnin *et al* 1984, 1985) amorphous alloys gives results very similar to Tb_xCu_{1-x}.

In the case of $Gd_{43}Al_{57}$ (Spano and Rhyne 1987) (Gd^{3+} is a S-state ion, without

Table 2. The $4\pi\,\mathrm{d}\sigma/\mathrm{d}\omega$ experimental curves have been fitted by

$$A/(q^2+\kappa^2)^2 + B\exp(-Cq) + E\exp(-Fq^2) \quad (2)$$

or

$$A/(q^2+\kappa^2)^{3/2} + B\exp(-Cq) + E\exp(-Fq^2) \quad (3)$$

The first term for small κ values, of $L^{N/2}$ type, can also be replaced by a q^{-N} power law. The samples are characterized by ZFC (zero-field-cooled) and FC (field-cooled) and asteriks indicates the use of equation (3) ($L^{3/2}$). The table gives the parameters values for equations (2) and (3) adjusted to the normalized scattering curves expressed in μ_B^2/RE for $T < 220$ K and in b/RE for higher temperatures. The parameters C, κ ($= 1/\xi$) and $\sqrt{F}$ are in units of $\mathrm{\AA}^{-1}$. The experimental exponent of the power law is reported in the column 'slope'. The parameter values given for the 4 K FC Tb alloy have been obtained from fitting equation (3) with intensities measured in a direction perpendicular to the magnetic field. For $T = 4$ K, ZFC, a Lorentzian-squared function L^2 describes the low q data better, because of observed saturation at low q values. The nuclear scattering is about 10^{-3} times the magnetic saturation (if both are expressed in the same units), but obeys the same laws.

Alloy	A	κ	B	C	E	F	Slope
$Tb_{65}Cu_{35}$							
4 K ZFC	0.08	4.2×10^{-3}	3×10^5	22	1.2×10^4	20	~ -4
4 K FC*	0.13	7×10^{-4}	1×10^5	20	5×10^3	10	−2.86
60 K FC	0.02	2.1×10^{-3}	6×10^5	40	1.2×10^4	20	−3.54
110 K FC*	0.015	6×10^{-4}	1×10^5	58	2×10^3	12	−2.48
220 K	8.7×10^{-6}	6×10^{-4}	7.3×10^2	50	58	70	−3.89
$Er_{69.5}Cu_{30.5}$							
5 K ZFC*	0.07	3×10^{-4}	4×10^4	17	4×10^3	10	—
300 K	4.4×10^{-6}	4×10^{-4}	7.3×10^3	250	7.3×10^2	700–400	−3.47

anisotropy) two Lorentzian terms, L^2 and L', are needed to describe the scattering with very different correlation lengths ($\xi = 1/\kappa \sim 200$ Å and $\xi' \sim 14$ Å, respectively). The L^2 term has been related to the presence of relatively long-range ferromagnetic correlations which coexist with finite 'spin glass' clusters (L' term). Both terms vary differently with temperature. The finite static spin glass clusters have some similarity with the aggregates introduced for TbCu.

In DyCu (Pickart *et al* 1984) very small correlation lengths ($\xi = 1/\kappa \sim 13$ Å) are detected. The temperature dependence of ξ shows that below 40 K and down to $T_f \sim 17$ K, ξ increases. At lower T values, ξ remains constant but spin polarization continues to increase.

3.3.3. Surface layer effects. When the sample surface is polished along a given direction with fine sandpaper, we observe a weak increase of the nuclear order; at 300 K a component varying as q^{-3} appears at the lowest q values, but is too weak to allow a quantitative description. However, the isotropic magnetic scattering (as detected at low T) is increased by a factor of 100 and two side peaks appear at very low q values along the polishing direction. This points to an important increase of bulk magnetic domain size and an antiferromagnetic ordering of surface layer domains, with a periodicity of ~ 4000 Å, the magnetization of a domain being perpendicular to the polishing direction. The thickness of the surface domains is about 1500 Å (figures 12–14). This surface layer effect has not been observed for $Er_{69}Cu_{31}$ (Boucher *et al* 1988b, c).

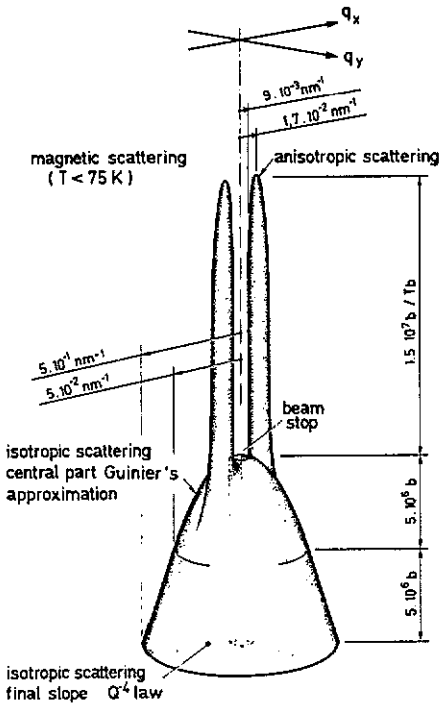

Figure 12. Schematic representation of SANS for a polished a-$Tb_{65}Cu_{35}$ sample. We observe at 4 K a very important isotropic scattering and two spectacular peaks which disappear either in applied field or above 110 K. No nuclear scattering peak has been detected.

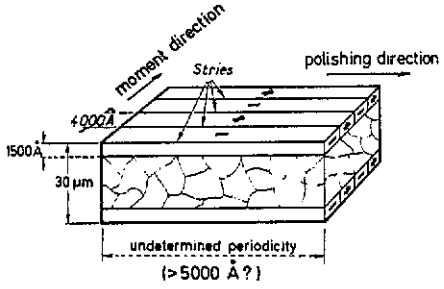

Figure 13. Schematic representation of the magnetic domains in an amorphous $Tb_{65}Cu_{35}$ sheet. The surface layer domain magnetizations are perpendicular to polishing direction and alternatively positively and negatively oriented.

3.3.4. Summary. The study of MRO in RE amorphous alloys with a magnetic ion provides evidence for

(i) the influence of nuclear order on the magnetic structure

(ii) the inhomogeneous distribution of atoms and of magnetizations (over distances from 10 to 10^3 Å and greater) and

(iii) the role of the surface layer on the magnetic MRO.

The 'seedy magnetic order' model illustrates the different scales of the inhomogeneties with the possibility of magnetic 'bubbles' formation in a matrix where the spin order is described by a CSG type model. With an applied field the scattering law is modified to give a MRO extending to greater distances and varying more sharply at small

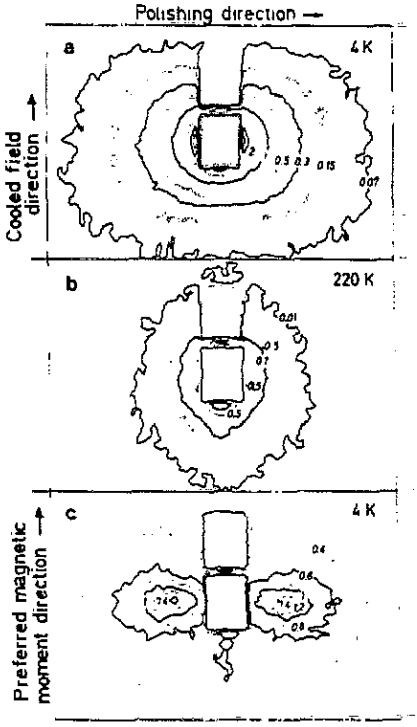

Figure 14. Isointensity curves of polished $Tb_{65}Cu_{35}$. The numbers represent isointensity values: (*a*) at 4 K, FC sample; (*b*) at 220 K ($\gg \theta$); (*c*) at 4 K after annealing at 220 K. The patterns were taken with two beam stops. The 220 K pattern is due to nuclear scattering and is really isotropic. The FC pattern is distorted by the field, the intensities being displaced towards low q values but does not present side peaks which are clearly visible in (*c*) (Boucher *et al* 1988b).

distances. A part of magnetic MRO subsists above the asymptotic Curie temperature, the magnetic order vanishing stepwisely in the different scales at which magnetic MRO is observed.

3.4. MRO in alloys with two magnetic ions (RE–3d alloys)

The amorphous RE–3d alloys are characterized by a magnetic ordering temperature above room temperature. Thus it is difficult to study the nuclear scattering by taking patterns above the magnetic ordering temperature because of the risks of sample crystallization. In these systems, the intensities are given in arbitrary scale and except for $ErCo_2$ (Boucher *et al* 1979b) only at few discrete q values, but the temperature and applied field dependence have been extensively studied, leading to a rather good agreement with the theory and confirming in particular that the magnetic clusters are finite.

A typical example illustrating the agreement with theoretical prediction is obtained by Rhyne (1987) for $TbFe_2$. When T tends to T_c from above, a conventional ferromagnet behaviour is observed with Lorentzian scattering and correlation length $\xi = 1/\kappa$. At $T = T_c$, the intensity at a given q value, does not present a maximum but an inflection, then for decreasing temperature it continues to increase showing that the alloy is not an ideal ferromagnet and a $L^2 + L'$ behaviour is observed (figure 15).

3.4.1. Lorentzian coefficients. Figure 16 shows the temperature dependence of the Lorentzian coefficients. A/κ varies as M^2 indicating that L^2 corresponds to the ordered part of the moments. But the authors underline that the behaviour of B (co-

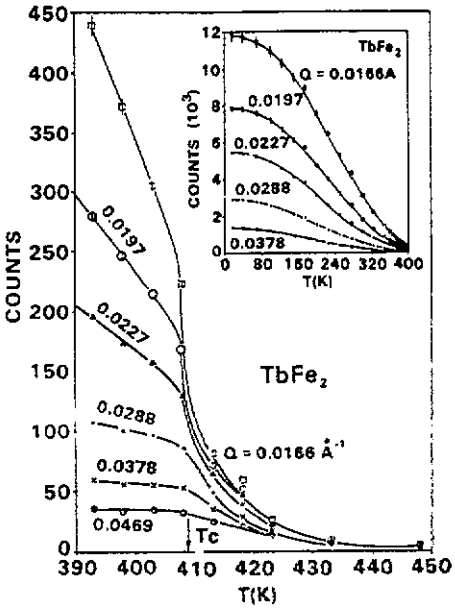

Figure 15. SANS intensity versus temperature for several discrete q values in $TbFe_2$ (Rhyne 1985).

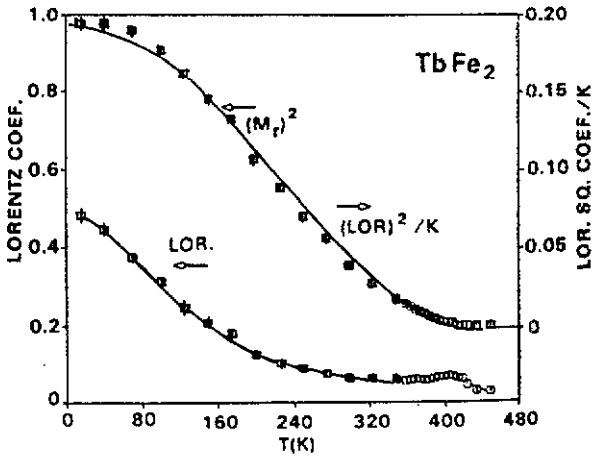

Figure 16. Temperature dependence of Lorentzian coefficient and Lorentzian-squared coefficient ($\propto A/\kappa$) for $TbFe_2$. The points represent the experimental values. A/κ is closely proportional to the field-induced magnetization squared extrapoled to $H = 0$ (full curve) (Rhyne 1986).

efficient of L') which 'mimics' the M^2 variations represents, at least partially, static variations and not only the spin waves and residual spin fluctuations as from theory.

3.4.2. Temperature dependence of ξ (figure 17). ξ exhibits a finite maximum ($\sim$ 100 –200 Å) at T_c which increases with the percentage of RE and goes down to a plateau ($\xi \sim 50$ Å) independent of RE content at lower T values.

This finite maximum has the shape of a cusp due to the anisotropy (RAM) or of a rounded maximum (RFM) due to positive and negative competing magnetic inter-

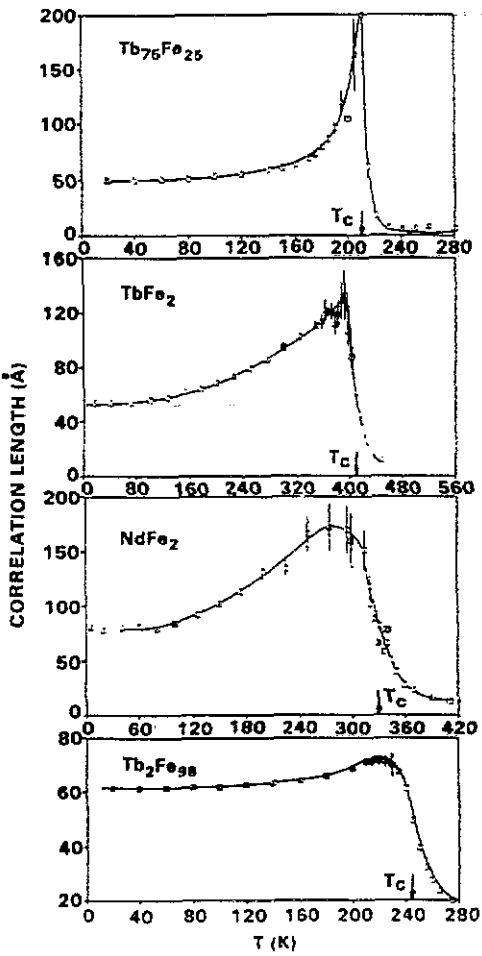

Figure 17. Temperature dependence of the spin correlation length ξ (Rhyne 1985).

actions (e.g. for small percentage of RE: Tb_2Fe_{98}). In the last case we have rather a freezing temperature T_f. The 'plateau' is due to the increase of anisotropy or random field when the temperature decreases which destroys the ferromagnetic order, and tends to reduce the correlation length. The authors conclude to the existence of finite magnetic cluster.

3.4.3. Field dependence of the correlation length ξ_T corresponding to the transverse part of the cross section in $TbFe_2$. On increasing the applied field the scattering increases at the lowest q values and is elliptically distorted because of the induced preferred moment direction as in figure 14(a). For a given q value, we would expect a more intense scattering $I(q)$ in a plane perpendicular to the field (in the case of a ferromagnet), but the opposite is observed. The authors assume that increasing field induces a nearly infinite percolating cluster which scatters at very low q values, e.g. at the limit of the measured q range, and invoke a super-paramagnetic-like response for the residual (Rhyne 1985). In this case, Chudnovsky (1988) has shown that ξ_T should vary as $1/\sqrt{H}$, which is what the measurements seem to confirm (figure 18).

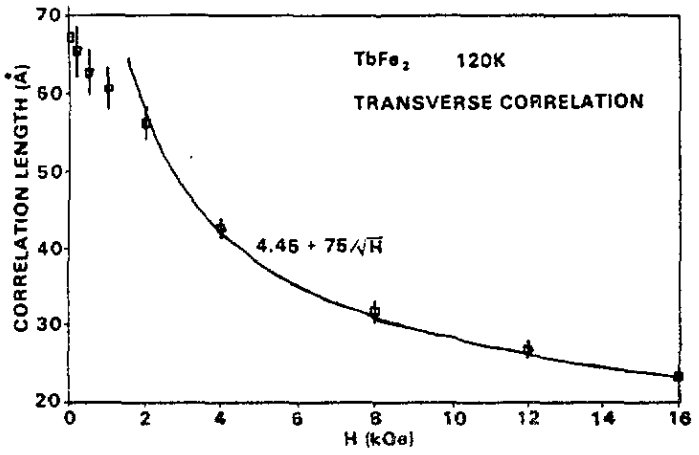

Figure 18. Field dependence of the transverse correlation length. The full curve is the theoretical $1/\sqrt{H}$ dependence, the points are experimental values (Rhyne 1985).

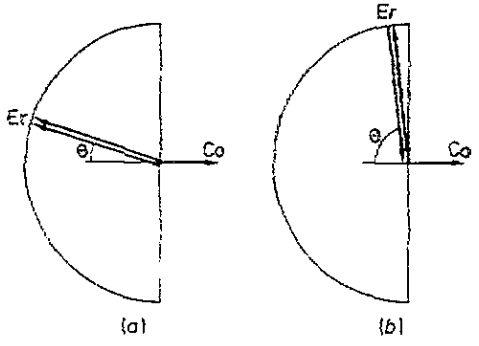

Figure 19. Schematic representation of MRO for $ErCo_2$. The Co moments are parallel over large distance. The (*a*) ferromagnetic and (*b*) antiferromagnetic arrangements of the Er moments depend on the angle between the Co moment and the Er moment directions, the latter being determined by the local axis of easy magnetization (Boucher *et al* 1979a).

3.4.4. Role of the 3d magnetic ion. The role of the 3d ion has not yet been separately considered. The $ErCo_2$ alloy (Boucher *et al* 1979a,b) gives some indication of the importance of 3d ions. In this alloy, the Co moments are parallel over relatively large distances giving rise to large domains ($2\pi/q \sim 10^3$ Å). On the other hand, the directions of easy magnetization which are produced by the nuclear ordering and which induce the Er moment directions, are correlated over distances of $2\pi/q \sim 200$ Å. Depending on the average Er moment direction with respect to that of Co, we distinguish two subdomains. The Er moments are in average, either all pointing in the same direction opposite to the Co moment, or they are antiparallel and make a large angle with the Co moment direction (figure 19). With applied field the size of the large domains increases, while the 'subdomains' are unchanged, the cobalt magnetization having already, for $H = 0$ induced the Er moment order. This result which is due both to the competition between the exchange interactions Co–Er and Er–Er and to

the nuclear MRO of the easy magnetization axis, is in agreement with suggestions of J M Dubois (1988) concerning the arrangements of polyedra in disordered alloys and is a good illustration of the role played by the 3d ions.

For the Fe-rich Tb–Fe alloys (Rhyne 1985), we are in different situation where the competing magnetic interactions lead to a dispersion of Fe moments and to a distribution of freezing temperatures. Indeed in $NdFe_2$ no special order and in particular no correlation between the easy magnetization axis has been detected (Pickart *et al* 1986).

3.4.5. Summary. In the RE–3d alloys:

(i) for $T > T_c$ spin fluctuations are observed with Lorentzian scattering curve as in conventional ferromagnets;

(ii) the measurements do not show evidence for a divergence of ξ when $T \rightarrow T_c$ from above; the existence of finite clusters is confirmed;

(iii) for $T < T_c$, a scattering curve sharply varying at low q values is observed, indicating a rather long distance magnetic order although, with decreasing temperature, ξ is reduced as expected from the increasing perturbation of the magnetic ordering due to disorder, predicted by the RAM or RFM;

(iv) an applied field increases the domain sizes while some small domains induce a superparamagnetic behaviour;

(v) the second magnetic ion (3d ion) can influence strongly the magnetic order, introducing small domains and leading to a distribution of freezing temperature rounding the cusp observed in $\xi(T)$.

4. Discussion

We have seen that both a strictly phenomenological analysis of the experimental results and an analysis guided by the prevailing theories converge to a simple set of scattering laws such as $L^{N/2}$, q^{-N} or $\exp(-\alpha q^2)$, $\exp(-\beta q)$ which are sufficient to describe completely the SANS data observed. Considering the variety of the investigated systems and the complexity of amorphous alloy preparation and characterization, this is in itself an interesting result. From these scattering laws, we can extract the correlation length of the fluctuations (or the size of the clusters or aggregates). Each law corresponds also to a real-space profile of the contrast for scattering and, in the case of absolute intensity measurement, allows us to reach the averaged effective concentration or magnetization in a given microscopic or mesoscopic volume.

A series of conclusions can therefore be drawn.

At temperatures below the ordering temperature T_c (or T_f), which is not a very well adapted concept since it is difficult to unambiguously define a critical temperature in these systems, it is evident that the scattering is not of a Lorentzian type. A scattering law such as L^2+L' (or a q^{-4} law) is then found, the L^2 term being predicted by analogy with spin glass and power laws being expected from renormalization theories; but $L^{3/2}$ or q^{-3} laws have also been encountered and were interpreted as being due to either a particular magnetization profile or a particular distribution of cluster sizes (Rhyne *et al* 1988).

Above the ordering temperature, there are cases, such as for Tb_xFe_{1-x}, where a Lorentzian magnetic scattering is observed as in conventional ferromagnets; but we

might also simply observe a progressive disappearance of the low temperature law (e.g. Tb_xCu_{1-x}).

At the difference of a conventional ferromagnet, the temperature dependence of the correlation length for magnetic fluctuations does not diverge at the approach of the ordering temperature, but always remains finite, confirming that random anistropy (or random field) prevents the existence of an infinite magnetic cluster. However, an applied field leads to partial percolation of the finite magnetic clusters, it distorts the isotropy of the scattering and decreases the correlation transverse to the field ξ_T, which varies as $1/\sqrt{H}$ as predicted. The temperature dependence of the magnetic MRO allows us to better understand the difficulty in defining an ordering temperature since the decoupling between the magnetizations of the large domains is observed at a lower temperature than that of aggregates of smaller size. So, for a given MRO, it is natural to obtain different ordering temperatures depending on the detection method (magnetization, SANS, neutron depolarization, etc.).

In the case of one magnetic RE ion, where the ordering temperature is low enough to explore the nuclear MRO, it is found that nuclear scattering is described by the same formal expression as the magnetic one, showing that the magnetic order essentially replicates and reveals the nuclear MRO. This is an important finding since fast quenched materials have far-from-equilibrium atomic distributions and coarse structure due to nanosegregation or quenched fluctuations is observed. However, magnetic fluctuations lead sometimes to new order such as the creation of small magnetic domain in the large nuclear ones (e.g. $Tb_{0.65}Cu_{0.35}$).

The above conclusions show that the amorphous magnetic alloys are generally not randomly disordered but also that their ordering cannot be reduced to merely short-range order. A correct description of their MRO characteristics is essential for the understanding of their physical properties. In this respect, it is very important to accumulate sufficient observations on a given system and in particular to measure the nuclear as well as magnetic MRO over as extended a q range as possible. It is true that most of the scattering laws and corresponding models apply only to a well defined q range and display specific temperature or field dependence, but a global examination of the whole scattering pattern is necessary to find the q range characteristic of a given scattering law.

These problems having been mastered, one could strictly consider the scattering due to large domains where several questions remain unsolved. Lower q values than those accessed up to now should be reached in order to confirm the domain sizes and to detect the leveling off of the Lorentzian-squared law. On the theoretical side, the $L^2 + L'$ description of the large magnetic domains also needs to be clarified, since the L' term is introduced as a dynamic one but its coefficient varies experimentally as a magnetization squared, underlining a static character; moreover the correlations lengths of the L^2 and L' terms are either found to be identical or fully decoupled. More profound is the lack of understanding of the reasons leading in some cases to $L^{3/2}$ or q^{-3} laws instead of $L^2 + L'$. We remind the reader that these laws are occasionally observed for nuclear as well as magnetic scattering and can be produced by an applied field (e.g. in $Tb_{0.65}Cu_{0.35}$ a $L^{3/2}$ law is observed with applied field, cf L^2 for $H = 0$). In this respect, the part played by surface effects which has been evidenced for some systems, seems not to be significant for the one-magnetic-ion case but further studies would be welcomed. Certainly, the systems that have been investigated up to now are satisfactorily described by one of the above laws, and the two types of models which have been developed (with well defined domain boundaries or with a specific profile for

the fluctuation) seem adequate. However, our knowledge remains too descriptive and is too fragmentory. On the experimental side, the restricted access to neutron beams, the need for very intense magnetic fields to overcome the anisotropy, the difficulties inherent to sample preparation and characterization, are real limitations. We believe, however, that a better understanding of the effects leading to the various $L^{N/2}$ or q^{-N} scattering laws, a better distinction between frozen-in compositional fluctuations or segregation (as perturbed by annealing) and disorder of purely magnetic origin (as perturbed by T, H, 3d ion) could throw some light not only on the magnetic but also on the nuclear MRO of these far-from-equilibrium disordered materials.

References

Aharony A and Pytte E 1980 *Phys. Rev. Lett.* **45** 1583
—— 1983 *Phys. Rev.* B **27** 5872
Alperin H A, Gillmor W R, Pickart S J and Rhyne J J 1979 *J. Appl. Phys.* **50** 1958
Boucher B 1977a *Phys. Status Solidi* **40** 197
—— 1977b *IEEE Trans. Magn.* **MAG-13** 1601
Boucher B, Chieux P, Convert P, Tourbot R and Tournarie M 1986 *J. Phys. F: Met. Phys.* **16** 1821
Boucher B, Chieux P, Convert P and Tournarie M 1983 *J. Phys. F: Met. Phys.* **13** 1339
Boucher B, Chieux P, Sanquer M and Tourbot R 1990a *J. Non-Cryst. Solids* **117/118** 191
Boucher B, Elgadi M, Sanquer M, Tourbot R, Bigot J, Chieux P, Convert P and Bellisent-Funel M C 1988a *Z. Phys. Chem., NF* **157** 23
Boucher B, Lienard A, Rebouillat J P and Schweizer J 1979a *J. Phys. F: Met. Phys.* **9** 1421
—— 1979b *J. Phys. F: Met. Phys.* **9** 1432
Boucher B, Sanquer M, Tourbot R and Chieux P 1988b *J. Physique Coll.* **49** C8 1727
Boucher B, Sanquer M, Tourbot R, Chieux P, Convert P, Maret M and Bigot J 1988c *Mater. Sci. Eng.* **99** 161
Boucher B, Sanquer M, Tourbot R, Chieux P and Maret M 1990b *J. Phys.: Condens. Matter* **1** 2647
Chappert J 1982 *Magnetism of Metals and Alloys* ed M Cyrot (Amsterdam: North-Holland)
Chudnosvky E M, Saslow W M and Serota R A 1986 *Phys. Rev.* B **33** 251
Chudnovsky E M 1988 *J. Appl. Phys.* **64** 5770
Dubois J M 1988 *J. Less-Common Met.* **145** 309
Fernandez-Baca J A, Rhyne J J, Erwin R W and Fish G E 1988 *J. Physique Coll.* **49** C8 1207
Fischer K H 1987 *Phys. Rev.* B **36** 6963
Flank A M and Naudon A 1980 *J. Physique Coll.* C8 123
Guimaraes D, Sanquer M, Tourbot R, Bellissent-Funel M C and Boucher B 1987 *Magnetic Properties of Amorphous Metals* ed A Hernando, V Madurza, M C Sanchez-Trujillo and M Varquez (Amsterdam: Elsevier)
Harris R, Plischke M and Zuckermann M J 1973 *Phys. Rev. Lett.* **31** 60
Hasanain S, Pickart S J and Nunes AC 1986 *J. Magn. Magn. Mater.* **54-57** 285
Imry Y and Ma S K 1975 *Phys. Rev. Lett.* **35** 1939
Lamparter P and Chieux P 1991 private communication
Lamparter P and Steeb S 1988 *J. Non-Cryst. Solids* **106** 137
Maret, Chieux P and Hicter P 1988 *Z. Phys. Chem., NF* **157** 109
Pappa B and Boucher B 1980 *J. Magn. Magn. Mater.* **15-18** 97
Pickart S J, Alperin H A, Gambino R J and McGuire T R 1984 *J. Appl. Phys.* **55** 1763
Pickart S J, Hasanian S, Shirane G and Majkrzak C F 1988 *J. Magn. Magn. Mater.* **58** 83
Pickart S J, Rhyne J J and Alperin H A 1974 *Phys. Rev. Lett.* **33** 424
Rhyne J J 1985 *IEEE Trans. Magn.* **MAG-21** 1990
—— 1986 *Physica* **136B** 30
—— J J 1987 *J. Magn. Magn. Mater.* **70** 88
Rhyne J J, Erwin R W, Fernandez-Baca J A and Fish G E 1988 *J. Appl. Phys.* **63** 4080
Rhyne J J and Glincka C J 1984 *J. Appl. Phys.* **55** 1691
Rhyne J J, Price D L and Mook H A 1974 *AIP Conf. Proc.* **24** 121
Rodmacq B, Mangin P and Chamberod A 1985 *J. Physique Coll.* **46** C8 499

Simonnin P 1984 *Thèse* Université Paris VI
Simonnin P, Tourbot R, Tournarie M and Boucher B 1985 *J. Phys. F: Met. Phys.* **15** L189
Spano M L, Alperin H A, Rhyne J J, Pickart S J, Hasanain S and Andrauska D 1985 *J. Appl. Phys.* **57** 3432
Spano M L and Rhyne J J 1985 *J. Appl. Phys.* **57** 3303
—— 1987 *J. Appl. Phys.* **61** 4100
—— 1988 *J. Appl. Phys.* **63** 3752
Spano M L, Rhyne J J, Pickart S J, Hasanain S K, Gambino R J and McGuire T R 1987 *J. Appl. Phys.* **61** 3639
Tomimitsu H, Kakahashi T, Kikuta S and Doi K 1986 *J. Non-Cryst. Solids* **88** 388–94
Wang Zhenxi, Yu Boliang, Wang Yizhong, Huang Jiao Hong, Yin Lin and Feng Minying 1988 *Mater. Sci. Eng.* **99** 123